Pure appl. geophys. 162 (2005) 1673–1688
0033 – 4553/05/091673–16
DOI 10.1007/s00024-005-2688-5

Pure and Applied Geophysics

Effect of the Mahanadi River on the Development of Storm Surge Along the Orissa Coast of India: A Numerical Study

S.K. Dube,[1,2] P.C. Sinha,[1] A.D. Rao,[1] Indu Jain,[1] and Neetu Agnihotri[1]

Abstract—River-ocean coupled models are described for the evaluation of the interaction between river discharge and surge development along the Orissa coast of India. The models are used to study the effect of fresh water discharge from the Mahanadi River on the surge response along the Orissa coast due to the October 1999 super cyclone which led to severe flooding of the coastal and delta regions of Orissa. The so-called 1999 Paradip cyclone was one of the most severe cyclones; causing extensive damage to property and loss of lives. The present study emphasizes the impact of the Mahanadi River on overall surge development along the Orissa coast. Therefore, we have developed a location specific fine resolution model for the Orissa coast and coupled it with a one–dimensional river model. The numerical experiments are carried out, both with and without inclusion of fresh water discharge from the river. The bathymetry for the model has been taken from the naval hydrographic charts extending from the south of Orissa to the south of west Bengal. A simple drying scheme has also been included in the model in order to avoid the exposure of land near the coast due to strong negative sea-surface elevations. The simulations with river-ocean coupled models show that the discharge of fresh water carried by the river may modify the surge height in the Bay, especially in the western Bay of Bengal where one of the largest river systems of the east coast of India, the Mahanadi River, joins with the Bay of Bengal. Another dynamic effect of this inlet is the potentially deep inland penetration of the surge originating in the Bay. The model results are in good agreement with the available observations/estimates.

Key words: Mahanadi River, Bay of Bengal, tropical cyclone, numerical model, storm surge, fresh water.

1. Introduction

The destruction caused by storm surges associated with severe cyclonic storms along the Indian coastline is of great concern (Dube *et al.*, 1997). The coastal regions of the state of Orissa (Fig. 1) occasionally experiences loss of life and severe damage to property from tropical cyclones originating in the Bay of Bengal (Murty *et al.*, 1986; Dube *et al.*, 1994, 1997, 2000a,b; Das *et al.*, 1983). The coastal districts of Orissa (Fig. 2) have experienced major surges in the past. Storm surges and the rains

[1] Centre for Atmospheric Sciences, Indian Institute of Technology, Hauz Khas, New Delhi 110 016, India.
[2] Indian Institute of Technology, Kharagpur, West Bengal 721 302, India.

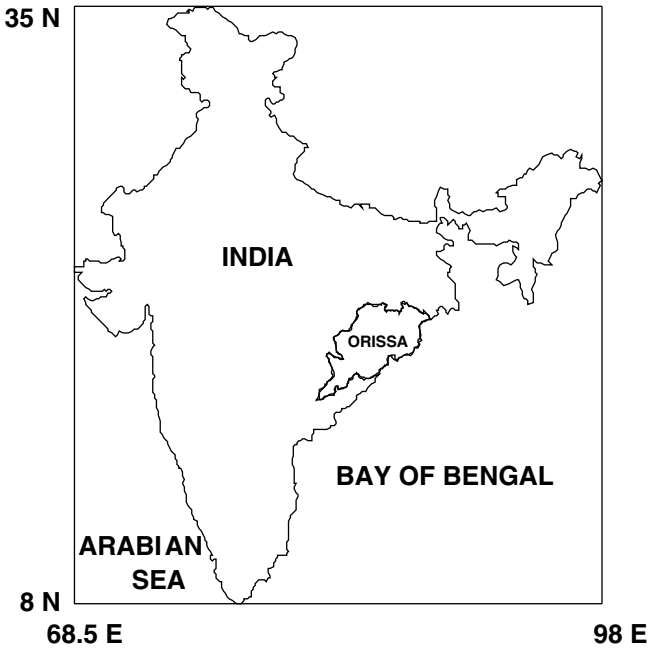

Figure 1
Bay of Bengal coast of India showing the location of the state of Orissa.

associated with the cyclones are major causes of coastal flooding in the region. Damage can be minimized if the storm surges are forecasted well in advance. RAO (1968) classified the Orissa coast in a category in which surges of around 3–5 m may be expected. The most vulnerable region is the coastal stretch between Puri and Balasore. It has been found that most of the severe cyclones in this region made landfall near Paradip.

DUBE *et al.* (1994) developed a real-time storm surge prediction system. Further improvements in the prediction system are carried out by developing a model on the regional scale for the Andhra coast (RAO *et al.*, 1997). In the present paper we have developed a location specific storm surge model for the Orissa coast (henceforth referred to as the bay model), which is vulnerable to inundation due to storm surges. The model runs on a personal computer. The analysis region extends from 18.25°N to 22°N and 84°E to 90°E (Fig. 2). We use the actual bathymetry from the naval hydrographic chart for the region extending from the south of Orissa to the south of west Bengal and a simple drying scheme has also been included in the model in order to avoid the exposure of land near the coast due to strong negative surges. The coastal boundary in this model has been taken as vertical side-walls through which there is no flux of water. However, the use of an idealized vertical side-wall may lead to a misrepresentation of the surge development.

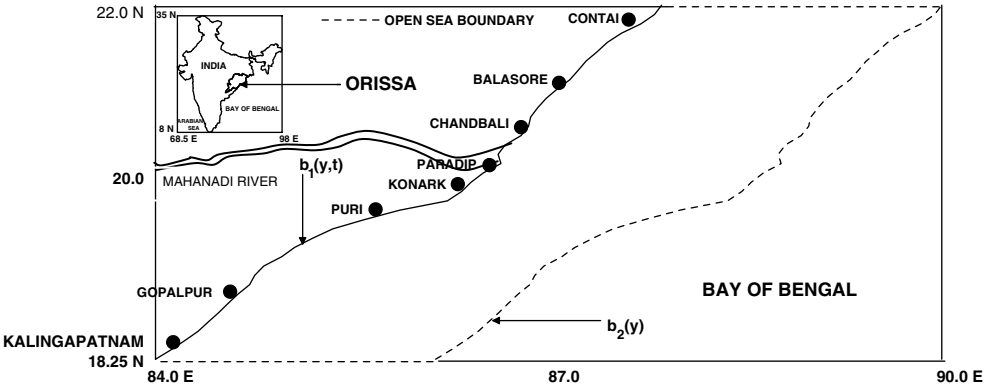

Figure 2
Map showing the Orissa coast and the analyzed region of the model.

Initially, the numerical model does not take into account the effect of any river or inlet joining the sea. This may result in an unrealistic high sea-surface elevation in the region where one of the largest river systems, the Mahanadi River, joins the Bay. Dynamically, this river system may be important for two reasons: (i) variations in the fresh water discharge may modify the surge height in the Bay, and (ii) the presence of such waterway allows a potentially deep inland penetration of the surge originating in the Bay.

Earlier, JOHNS and ALI (1980) developed a river-bay coupled model for the simulation of surges along the Bangladesh coast. In the present work we have modified the bay model by taking into account the effect of the River Mahanadi joining the Bay near Paradip. However, in contrast to the work of Johns and Ali (1980) our method does not depend on the patching together of computational regions with different uniform grid spacing. It is more similar to the work earlier reported by JOHNS *et al.* (1983) wherein a continuously contracting grid system is used to resolve the surge development along the Orissa coast of India. Another noteworthy difference in the formulation of our model from that of JOHNS and ALI (1980) is the way in which the topography of the Orissa coast is represented. The treatment of the coastal boundary involves a procedure leading to a realistic curvilinear representation of the natural shoreline.

Using this ocean-river coupled model, we have performed numerical experiments to simulate the surge generated by the October 1999 Orissa super cyclone. Comparison of the results of this model with those obtained from the bay model indicates that the surge height is significantly affected in the region where the river joins the Bay. Experiments are also performed to investigate the effect of fresh water discharge on the modification of surge height along the coast, and to estimate the extent of inland penetration of surge water through the river. Hence, simulations using both models, with and without inclusion of the river along the Orissa coast,

show that the incorporation of a river in the storm surge model leads to an important change in the prediction detail.

2. Basic Equations

For the formulation of the model a system of rectangular Cartesian coordinates are used in which the origin, O, is within the equilibrium level of the free surface. Ox points towards the east, Oy towards the north and Oz is directed vertically upwards. The displaced position of the free surface is given by $z = \zeta(x, y, t)$ and the position of the sea floor by $z = -h(x,y)$. A western coastal boundary (the east coast of India is situated at $x = b_1(y)$ and an eastern open sea boundary is situated at $x = b_2(y)$. Southern and northern open sea boundaries are at $y = 0$ and $y = L$, respectively. The treatment of the boundaries involves a procedure leading to a realistic curvilinear representation of both the western and the eastern sides of the analysis region (Fig. 2).

The depth-averaged equations of continuity and momentum for the dynamical processes in the western Bay, after neglecting barometric forcing and tide generating forces, are given in the flux form by

$$\frac{\partial \zeta}{\partial t} + \frac{\partial \tilde{u}}{\partial x} + \frac{\partial \tilde{v}}{\partial y} = 0 \tag{1}$$

$$\frac{\partial \tilde{u}}{\partial t} + \frac{\partial}{\partial x}(u\tilde{u}) + \frac{\partial}{\partial y}(v\tilde{u}) - f\tilde{v} = -g(\zeta + h)\frac{\partial \zeta}{\partial x} + \frac{F_s}{\rho} - \frac{c_f \tilde{u}}{(\zeta + h)}(u^2 + v^2)^{\frac{1}{2}} \tag{2}$$

$$\frac{\partial \tilde{v}}{\partial t} + \frac{\partial}{\partial x}(u\tilde{v}) + \frac{\partial}{\partial y}(v\tilde{v}) + f\tilde{u} = -g(\zeta + h)\frac{\partial \zeta}{\partial y} + \frac{G_s}{\rho} - \frac{c_f \tilde{v}}{(\zeta + h)}(u^2 + v^2)^{\frac{1}{2}} \tag{3}$$

where,

$$(\tilde{u}, \tilde{v}) = (\zeta + h)(u, v)$$

u, v :depth-averaged component of velocity in the direction of x, y respectively,
ζ :sea-surface elevation above the mean water level,
h :water depth,
t :time,
ρ :density of the seawater,
f :Coriolis parameter ($= 2\omega \sin \phi$),
g :acceleration due to gravity,
F_S, G_S :x and y components of the surface wind stress,
c_f :bottom friction coefficient ($= 2.6 \times 10^{-3}$)

The surface stresses are parameterized by a conventional quadratic law as follows

$$(F_s, G_s) = c_d \rho_a (u_a^2 + v_a^2)^{\frac{1}{2}}(u_a, v_a)$$

where $c_d = 2.8 \times 10^{-3}$ is the surface drag coefficient, ρ_a is the density of the air and u_a, v_a are the x and y components of the surface wind.

3. Boundary Conditions

The boundary condition at the western coastal boundary which is a vertical side-wall, is given by

$$u - v\frac{\partial b_1}{\partial y} = 0 \quad \text{at} \quad x = b_1(y). \tag{4}$$

At the eastern open sea boundary, a radiation condition is applied similar to that used by JOHNS *et al.* (1981). This leads to

$$u - v\frac{\partial b_2}{\partial y} - \left(\frac{g}{h}\right)^{\frac{1}{2}}\zeta = 0 \quad \text{at} \quad x = b_2(y). \tag{5}$$

Conceptually similar radiation conditions are applied at the southern and northern open sea boundaries to yield

$$v + \left(\frac{g}{h}\right)^{\frac{1}{2}}\zeta = 0 \quad \text{at} \quad y = 0, \tag{6}$$

$$v - \left(\frac{g}{h}\right)^{\frac{1}{2}}\zeta = 0 \quad \text{at} \quad y = L. \tag{7}$$

Further, a curvilinear representation of the coastal boundaries has been carried out, similar to the work by DUBE *et al* . (1994).

4. Fine Grid Resolution Adjacent to the Coast

Increased resolution near the coast is important to represent the topography more realistically. Since the location of the first off-shore point influence computation of the surge, more accuracy in prediction can be achieved by increasing the resolution near the coast. This can be done by further transformation of ξ coordinate. This is achieved by defining a new variable η by

$$\eta = \xi + \varepsilon \ln\left(\frac{\xi + \xi_0}{\xi_0}\right), \tag{8}$$

where $\xi = (x - b_1(y))/b(y)$, $b(y) = b_2(y) - b_1(y)$, and ε and ξ_0 are disposable parameters.

By virtue of equation (8) the increments $\Delta\xi$ and $\Delta\eta$ are related by

$$\Delta\xi = \frac{\Delta\eta}{1 + \varepsilon/(\xi + \xi_0)} \tag{9}$$

If we consider a uniform value of $\Delta\eta$ and take $\varepsilon = 0.04$ and $\xi_0 = 0.001$,

$\Delta\eta \to 0$, so that

$$(\Delta\xi)_{\xi=0.0} \cong (0.024)\Delta\eta,$$
$$(\Delta\xi)_{\xi=0.5} \cong (0.0926)\Delta\eta,$$
$$(\Delta\xi)_{\xi=1.0} \cong (0.0962)\Delta\eta.$$

Thus, near the coastline, the transformation (8) will lead to a substantial mesh refinement in which the grid increment is reduced to a fraction of its essentially uniform value between $\xi = 0.5$ and $\xi = 1.0$. Therefore, the use of equation (8) in equations (1)–(3) will assist in the incorporation of a more detailed bathymetric specification in the important coastal region. It must, however, be emphasized that the use of such a transformation is not without attendant danger. Equation (8) would be a natural transformation to use if the solution were known to have an almost linear dependence on ζ. This, of course, is not necessarily the case and an injudicious choice of values for ε and ξ_0 could lead to results contaminated by a substantial truncation error.

Writing

$$\frac{\partial\xi}{\partial\eta} = F(\eta) = \frac{1}{1+\varepsilon/(\xi+\xi_0)} \tag{10}$$

equations (1)–(3) take the form

$$\frac{\partial}{\partial t}(b\zeta) + \frac{1}{F}\frac{\partial}{\partial\eta}(bHU) + \frac{\partial}{\partial y}(bHv) = 0 \tag{11}$$

$$\frac{\partial\tilde{u}}{\partial t} + \frac{1}{F}\frac{\partial}{\partial\eta}(U\tilde{u}) + \frac{\partial}{\partial y}(v\tilde{u}) - f\tilde{v} = -\frac{gH}{F}\frac{\partial\zeta}{\partial\eta} + \frac{bF_S}{\rho} - \frac{c_f\tilde{u}}{H}(u^2+v^2)^{\frac{1}{2}} \tag{12}$$

$$\begin{aligned}&\frac{\partial\tilde{v}}{\partial t} + \frac{1}{F}\frac{\partial}{\partial\eta}(U\tilde{v}) + \frac{\partial}{\partial y}(v\tilde{v}) + f\tilde{u}\\ &= -gH\left[\frac{b\partial\zeta}{\partial y} - \left(\frac{\partial b_1}{\partial y} + \xi\frac{\partial b}{\partial y}\right)\frac{1}{F}\frac{\partial\zeta}{\partial\eta}\right] + \frac{bG_s}{\rho} - \frac{c_f\tilde{v}}{H}(u^2+v^2)^{\frac{1}{2}}\end{aligned} \tag{13}$$

where U is the velocity normal to the coastline and is given by

$$U = \frac{1}{b(y)}\left[u - \left(\frac{\partial b_1}{\partial y} + \xi\frac{\partial b}{\partial y}\right)v\right] \tag{14}$$

with $\tilde{u} = Hbu, \tilde{v} = Hbv, H = \zeta + h$.

A conditionally stable semi-explicit finite difference scheme with staggered grid is used for the numerical solution of the model equations. The staggered grid consists of three distinct types of computational points on which the sea-surface elevations and the zonal and meridional components of depth-averaged currents are computed. Following SIELECKI (1968), the computational stability is achieved by satisfying the

CFL (Courant-Friedrich-Lewy) criterion. In the present model this condition is satisfied by limiting the time step of integration to three minutes.

The bottom stress is computed from the depth-averaged currents using the conventional quadratic law with a constant coefficient of 0.0026. This value has been achieved by performing several numerical experiments (JOHNS *et al.*, 1983).

The bathymetry for the model is derived from the Naval Hydrographic Charts and is interpolated at the model grid points by using a cubic spline interpolation scheme. With this procedure, sufficiently accurate and realistic bathymetry is generated. A simple drying scheme has also been included in the model to avoid the exposure of land near the coast due to strong negative surges.

5. The River Model

The Mahanadi River is the sixth largest among the 14 major rivers of India that traverses and spreads over the states of Madhya Pradesh, Bihar, Maharashtra and Orissa before joining the Bay of Bengal. The river is 857 km long with a drainage area of 141,600 km^2 and accounts for 4.3% of the total area of the country. The depth of the river varies from 2–12 m. It extends between 80°30′E and 86°45′E longitudes; 19°20′N and 23°35′N latitudes. RAO (1990) suggested that the monthly stream flow data vary greatly; the largest value being in August and smallest during pre-monsoon months.

The Mahanadi estuarine region is determined by the extent of penetration of saline water, which depends on the season and different phases of the semidiurnal tide. It is observed that the distance of penetration of salt water varies from 25 to 35 km from the mouth, depending on the season. Hence the river channel is modelled by considering its length, ℓ, to be about 30 km upto which saline water intrusion is prevalent, neglecting other tributaries (Fig. 2). The breadth and mean depth are based on the data available from the Survey of India (SOI). Numerical experiments are performed for the river during the month of October. The channel has 36 uniform computational points in the horizontal with the grid increment (Δx) of 857 m and the time step has been taken as 90s. The freshwater discharge, Q, at the head of the river is specified to be 32, 376 $m^3 s^{-1}$ (ADSORBS, 1993–94). The same depth has been ensured for the common grid point of the river and the bay models.

The river is modelled as a channel with a variable but prescribed rectangular cross section with a flow that is assumed to be unidirectional. It is a 1-D barotropic depth-averaged numerical model. In the western Bay of Bengal the Mahanadi River connects with the main analysis area whose configuration is shown in Fig. 2. Following JOHNS and HAMZAH (1968), the meanders of the river have not been considered in the present model. However, in order to take into account the actual breadth of the river it is assumed that the x-axis is chosen in such a way that it is equidistant from either side of the river banks. The direct action of the meteoro-

logical and astronomical influences is ignored. The origin, O, is taken in the equilibrium level of the free surface and is located at the mouth of the river at $x = 0$. The landward end is denoted by $x = \ell$. The axis Ox is directed towards the west and Oz is directed vertically upwards. The elevation of the free-surface above its mean undisturbed level is denoted by $z = \zeta(x, t)$ and the bottom topography by $z = -h(x)$. The depth-averaged velocity, u, in the river then satisfies

$$B\frac{\partial \zeta}{\partial t} + \frac{\partial}{\partial x}(BHu) = 0 \tag{15}$$

and

$$\frac{\partial}{\partial t}(BHu) + \frac{\partial}{\partial x}(BHu^2) = -gBH\frac{\partial \zeta}{\partial x} - Bc_f u|u|, \tag{16}$$

where $B(x)$ is the breadth of the river at x. The bottom stress has been parameterized by a conventional quadric law $\rho c_f u|u|$. At the free surface the applied surface wind stress is taken as zero.

Dynamical conditions in the Mahanadi River are determined from equations (15) and (16). In order to generate the motion in the river the forcing is prescribed from the bay model, in the form of surge height at the river mouth.

5.1 Matching Conditions

The precise way in which the matching conditions between the bay and the river at the river mouth is accomplished, is important because of the transition from a fully two-dimensional bay model to a one-dimensional river model. The appropriate matching conditions at the river-bay junction are

$$\zeta_{\text{bay}} = \zeta_{\text{river}} \tag{17}$$

$$u_{\text{bay}} - v_{\text{bay}}\frac{\partial b_1}{\partial y} + u_{\text{river}}\left(1 + \left(\frac{\partial b_1}{\partial y}\right)^2\right)^{-1/2} = 0. \tag{18}$$

Equation (17) implies continuity of sea-surface elevation across the section while (18) ensures continuity of the volume flux. Similar matching conditions of surface continuity and volume continuity have also been used by JOHNS and ALI (1980).

5.2 Boundary and Initial Conditions for the River Model

At the river head we have considered two types of conditions. Either

$$u = 0 \tag{19}$$

when no fresh water input is considered, or

$$u = \frac{Q}{BH} \tag{20}$$

when the fresh water discharge is considered. Here, Q denotes the volume of fresh water entering the river per unit time, and it may be a constant or a prescribed function of time.

The matching condition (17) and boundary conditions (4) and (5) take the form

$$bU + u_{\text{river}}\left(1 + \left(\frac{\partial b_1}{\partial y}\right)^2\right)^{-1/2} = 0 \quad \text{at the bay-river junction} \tag{21}$$

$$U = 0 \quad \text{at} \quad \eta = 0 \tag{22}$$

and

$$bU - \left(\frac{g}{h}\right)^{1/2}\zeta = 0 \quad \text{at} \quad \eta = \eta_m \tag{23}$$

where

$$\eta_m = 1 + \varepsilon \ln\left(1 + \frac{1}{\zeta_0}\right). \tag{24}$$

6. Numerical Procedure

The grid points for the river model are on the x-axis which runs along the middle of the river. There are two kinds of grid points for the river. When i is odd the point is ζ- point at which ζ is computed. When i is even, the point is a u-point at which u is computed. The river mouth is represented by a ζ-point while the river head is given by a u-point. The depth h and the breadth B are prescribed at both types of points.

In the bay model the computations are performed on a staggered grid consisting of three distinct types of grid points. When i is even and j is odd, the point is a ζ-point at which elevation is computed. If i is odd and j is odd, the point is a u-point at which both u and U are computed, and finally when both i and j are even, the point is a v-point at which v is computed. Along $\eta = 0$, there will be only u-points and at each of these points $U = 0$ identically, except at the grid point on the mouth of the river where the continuity of volume flux is ensured. We choose m to be even so that $\eta = \eta_m$ consists of both ζ-points and v-points. We also choose n to be odd thus ensuring that there are only ζ-points and u-points along $y = 0$ and $y = L$. The factor $F(\eta)$ is evaluated at each of the discrete η-points by applying a Newton-Raphson iterative procedure. The corresponding discrete values of $F(\eta)$ are derived from (10).

Equations (15) and (16) yield procedures for updating elevation and current in the Mahanadi River. The value of ζ at the head of the river is extrapolated from the interior. The solution developed by this process must match the solution of the bay model. With a forcing applied at the mouth, the river model can be operated independently of the bay model.

6.1 Matching of the River Model with the Bay Model

For the solution process in the river model, the extrapolated value of the elevation from the bay model at the bay-river junction (referred to as the pivot point) provides a forcing for the motion in the river. The use of equations (15) and (16) leads to updated elevations and currents at the ζ- and u-points in the river, except for the current at the head of the river where the u-velocity is given by one of the boundary conditions (19) and (20). The updated elevation at the pivot point from the river model is chosen to update the elevations in the bay model by using condition (17) for the next iteration.

Using the current computed at the first u-point of the river, the boundary values of U may be determined for the bay model. This must be consistent with (21) which is replaced by

$$(U)_{\eta=0} = -\frac{1}{b}\left(u_{\text{river}}\right)_{x=\Delta x}\left(1+\left(\frac{\partial b_1}{\partial y}\right)^2\right)^{-1/2}. \tag{25}$$

By making use of the previously updated (or initial) elevations in the bay model, this matching procedure leads to updated elevations in the river and, additionally, yields boundary values of U across the mouth of the river to be used in the next updating of the bay model variables.

7. Numerical Experiments

In the present study numerical experiments have been first performed with a location specific storm surge model (bay model) for the Orissa coast having an idealized vertical side-wall. Next, numerical experiments have been conducted with a model in which the River Mahanadi joins the above-mentioned bay model near Paradip. Here, two experiments have been conducted, with and without river discharge from the upstream station, and their effect on the surge development along the coast has been analyzed. For both the models, without river and with river (for the case when the fresh water discharge is excluded), we prescribe an initial state of rest and integrate the governing equations (11)–(13), (15) and (16) ahead in time upto a total of 36 hours.

When fresh water discharge is taken into account in the river-bay model, the preliminary integration of the model equations requires the establishment of initial conditions corresponding to the fresh water discharge. In order to achieve this, we first prescribe an initial state of rest and integrate the governing equations ahead in time upto a total of 150 hours in order to reach a steady-state with only the prescribed fresh water discharge and no wind stress at the sea surface. Defining this steady-state condition as the initial state, the cyclonic wind stress was subsequently

applied and the model was run for another 36 hours to obtain the final results. In all our experiments, a time-step of 3 minutes was found to be consistent with the computational stability.

Using both models, with and without the inclusion of river, numerical experiments are performed to simulate the surge heights associated with cyclonic storms which struck the Orissa coast during October, 1999. The track of the cyclone in the analysis region is shown in Fig. 3. India Meteorological Department (IMD) estimated a lowest pressure of 98 hPa and a radius of maximum wind of 40 km at landfall near Paradip. These data were used in the model to carry out numerical experimentation. The wind stress forcing for driving the models has been computed by using the storm model of JELESNIANSKI and TAYLOR (1973).

8. Results and Discussion

A depression formed in the Bay of Bengal near 12°N and 98.5°E at 0600 UTC of 25th October, 1999. It became a cyclonic storm in the early hours of the 26th and was located at 13.5°N and 96.5°E. The cyclone moved further in a northwesterly direction and lay centered at 16°N and 92°E. It became a severe cyclonic storm with a core of hurricane winds on the 27th at 0300 UTC. The cyclone further intensified into a very severe cyclonic storm and lay centered at 17.5°N and 89.5°E on the 28th. The surge prediction was carried out using the track given by IMD after the cyclone crossed a

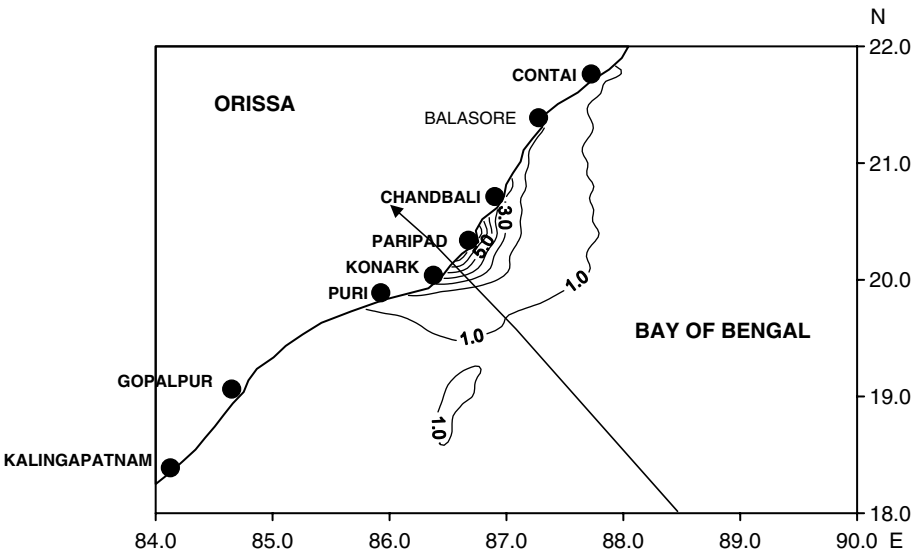

Figure 3
Surge contours (m) associated with 1999 Orissa cyclone and its track.

few km south of Paradip in Orissa. For numerical experiments, the starting point of the cyclone center is at 18°N and 88.5°E on the 29th of October at 0600 UTC.

Figure 3 delineates the computed surge contours along the Orissa coast using the bay model. It may be seen that the maximum surge of 7.7 m occurs to the right of the point of landfall. The coastal region between Konark and Chandbali is affected by a surge of more than 5 m. Post-storm survey reports of IMD also show that the surge was more than 7 m in proximity to Paradip.

In Fig. 4 we provide the distribution of the predicted maximum sea-surface elevation (peak surge envelope) along the Orissa coast using both models. The surge has been computed from the bay-river model both without and with fresh water discharge (henceforth referred to as MWD0 and MWD, respectively). The peak surge envelope for the bay model which does not include the river, henceforth referred to as BM, is also shown in Figure 4 for comparison. It can be seen that the maximum sea-surface elevations along the coast are the same except in the region near Paradip where the River Mahanadi joins the bay. MWD0 and MWD predict a maximum surge of 6.4 m and 6.5 m, respectively, at the river mouth where the predicted peak surge from BM is 6.8 m. Thus, the surge height computed by BM is higher than that obtained from MWD0 and MWD. This may presumably be attributed to the unrealistic accumulation of water near Paradip because of the assumption of an idealized vertical side-wall in BM. In MWD0 and MWD this piling up does not occur since the water is allowed to penetrate through the River Mahanadi thus reducing the maximum sea-surface elevation. A comparison of the results obtained from MWD0 and MWD indicates that the maximum surge predicted by the latter is about 10 cm higher at the river mouth. This may be due to the fact that the initial conditions corresponding to the fresh water discharge lead to a surface elevation above its equilibrium level in the river. We also note that the peak surge of 7.7 m occurs at the same position, P, in all three cases and the inclusion of the river has no impact on the peak surge, as the location of P is about 21 km away from the river mouth.

Fig. 5 presents a comparison of the temporal variation of the surge at the mouth of the Mahanadi River as computed from MWD0, MWD and BM. We note that BM yields, in general, a higher surge with a maximum difference of approximately 7% between 0002 UTC and 0330 UTC on 30th October, 1999. It may be seen that during the resurgence phase BM, MWD0 and MWD predict rapidly falling sea-surface elevations. However, MWD0 produces about 6% lower surge values compared to BM between 0700 UTC and 1800 UTC on 30th October, 1999. We also note that the computed phase difference between MWD0, MWD and BM is insignificant and the peak surge in the three cases occurs at about the same time.

The surface elevations in the Mahanadi River are also studied by integrating the model for 36 hours after steady state is reached in the case of MWD. Figure 6 provides an idea of the inland distance along the river upto which significant surface

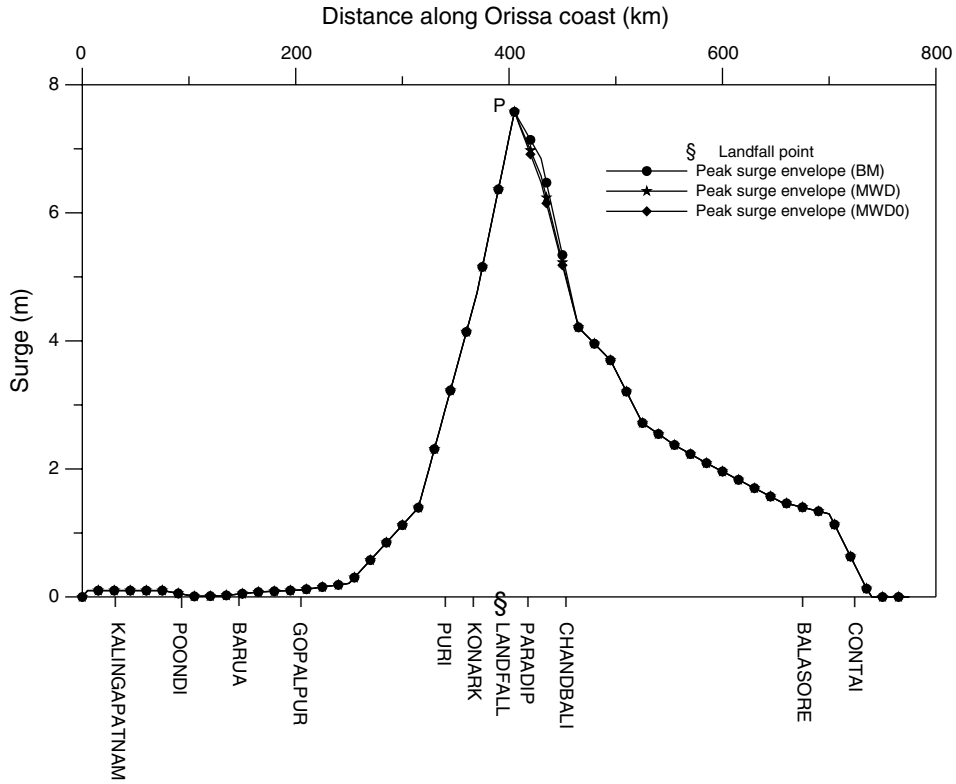

Figure 4
Peak surge envelope along the Orissa coast.

elevations may be expected, using both cases of with and without fresh water discharge at the river head.

It may be seen from Fig. 6 that the difference between the predicted surge response from MWD0 and MWD is insignificant upto a distance of about 8 km from the mouth of the river ($x = 0$). Further landward there is an appreciable difference between the results obtained from MWD0 and MWD with the former predicting lower values of peak surge than the latter all along the river. A maximum difference of 13% is seen at a landward distance of about 21 km. The surface elevation in the river is higher, in general, in the case of MWD as compared to MWD0. This may be due to the initial conditions corresponding to the fresh water discharge leading to a surface elevation above its equilibrium level.

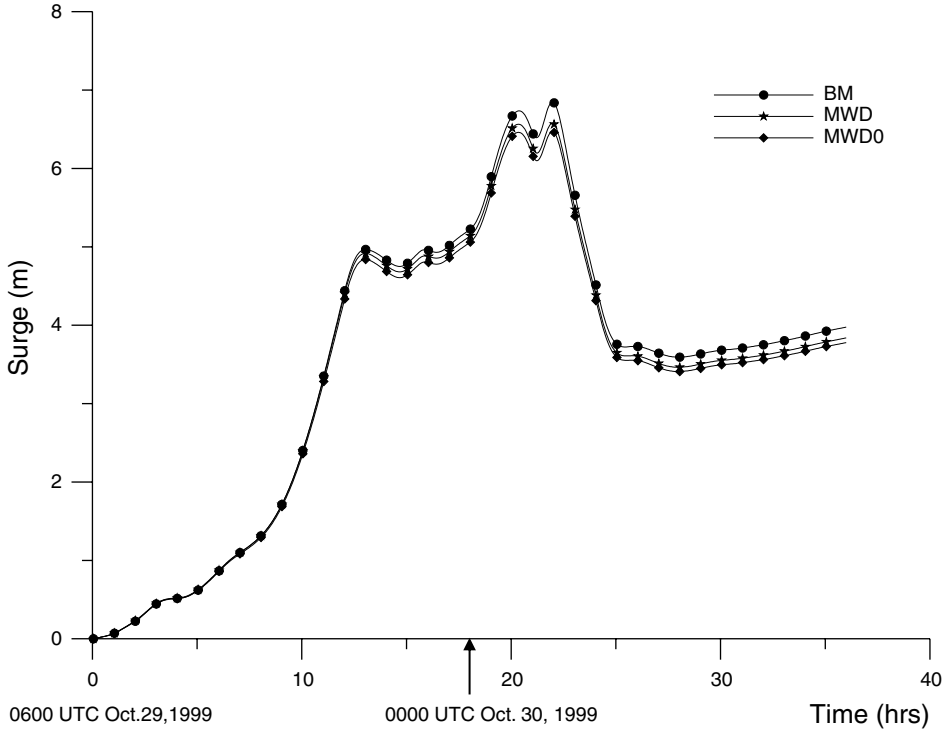

Figure 5
Temporal variation of the predicted surge (m) at the mouth of the Mahanadi River.

9. Conclusions

We have developed depth-averaged storm surge models for simulating the surges along the Orissa coast. Our analysis area includes a representation of the River Mahanadi. Using a forcing wind stress distribution representative of the 1999 Orissa super cyclone, a comparison is made between simulations using models both with and without inclusion of the river along the Orissa coast. The incorporation of a river in our model has shown that surge may penetrate inland, thus leading to a flooding hazard in the inland waterways of Orissa. It has also been shown that the surge response inside the river depends significantly upon the fresh water discharge. Thus, the response of the river on the surge development in the coastal and estuarine regions is appreciable and should be taken into account for any storm surge prediction study.

The model results reported in this study are in agreement with the available peak surge observations/estimates. The results emphasize the suitability of fine resolution location specific models for a reasonable prediction of surges along the Orissa coast.

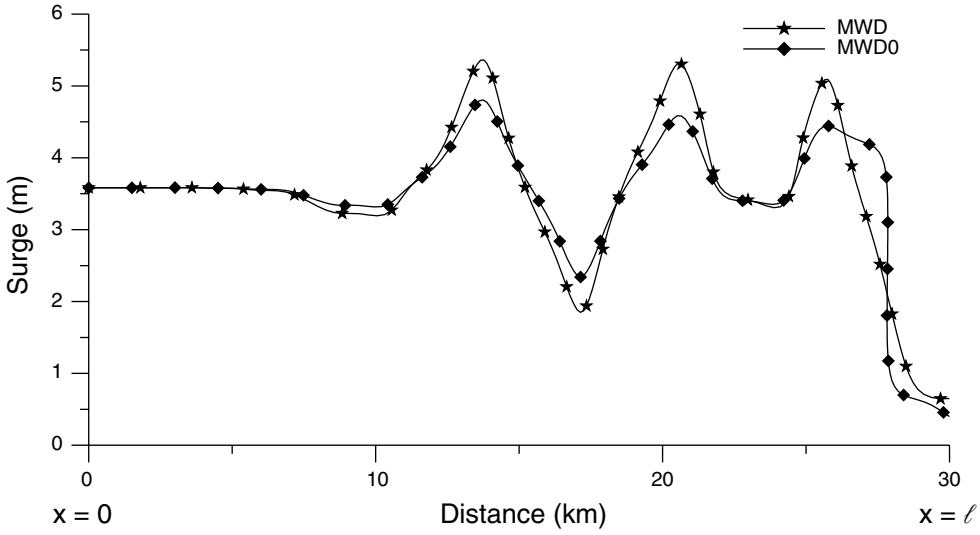

Figure 6
Predicted surface elevation (m) in the River Mahanadi.

In the present study, the cyclonic storm is the sole driving force for the dynamical processes in the sea. Tidal solution has not been used to provide the initial conditions for tide and surge interaction in the bay. Therefore, the nonlinear interaction of surge and the tide has not been considered in this study. Such an interaction may be significant if the occurrence of the surge coincides with that of the high tide. The model may be used for operational prediction of storm surges along the Orissa coast of India.

References

ADSORBS/23/1993–94 *Assessment and Development Study of River Basin Series*:, Central Pollution Control Board, Delhi, India.

DAS, P.K., DUBE, S.K., MOHANTY, U.C., SINHA, P.C., and RAO, A.D. (1983), *Numerical Simulation of the Surge Generated by the June 1982 Orissa Cyclone,* Mausam *34*, 359–366.

DUBE, S.K., RAO, A.D., SINHA, P.C., and CHITTIBABU, P. (1994), A *Real Time Storm Surge Prediction System: An Application to East Coast of India,* Proc. Indian Nat. Sci. Acad., *60*, 157–170.

DUBE, S.K., RAO, A.D., SINHA, P.C., MURTY, T.S., and BAHULAYAN, N. (1997), *Storm Surge in the Bay of Bengal and Arabian Sea: The Problem and its Prediction,* Mausam *48*, 283–304.

DUBE, S.K., CHITTIBABU, P., RAO, A.D., SINHA, P.C., and MURTY, T.S. (2000a), *Sea Levels and Coastal Inundation Due to Tropical Cyclones in Indian Coastal Regions of Andhra and Orissa,* Marine Geodesy *23*, 65–74.

DUBE, S.K., CHITTIBABU, P., RAO, A.D., SINHA, P.C., and MURTY, T.S. (2000b), *Extreme Sea Levels Associated with Severe Tropical Cyclones Hitting Orissa Coast of India,* Marine Geodesy *23*, 75–90.

JOHNS, B., and ALI, A. (1980), *The Numerical Modelling of Storm Surges in the Bay of Bengal,* Quart. J. Roy Met. Soc. *106*, 1–18.

JOHNS, B., DUBE, S.K., MOHANTY, U.C., and SINHA, P.C. (1981), *Numerical Simulation of the Surge Generated by the 1977 Andhra Cyclone,* Quart. J. Roy. Met. Soc. *107*, 915–934.

JOHNS, B. and HAMZA, A.M.O. (1968), *Long Standing Waves in a Curved Canal,* J. Fluid Mech. *34*, 759–768.

JOHNS, B., SINHA, P.C., DUBE , S.K., MOHANTY , U.C., and RAO , A.D. (1983), *Simulation of Storm Surges Using a Three-dimensional Numerical Model: An Application to the 1977 Andhra Cyclone,* Quart. J. Roy. Met. Soc. *109*, 211–224.

JELESNIANSKI, C.P. and TAYLOR, A.D. (1973), *NOAA Technical Memorandum,* ERL, WMPO-3, 33 pp.

MURTY, T.S., FLATHER, R.A., and HENRY, R.F. (1986), *The Storm Surge Problem in the Bay of Bengal,* Prog. Oceanog. *16*, 195–233.

RAO, N. S. B. (1968), *On Some Aspects of Local and Tropical Storms in the Indian Area,* Ph.D. Thesis, University of Jadavapur, India.

RAO, P.G. (1990), *Some Stream Flow Characteristics of the Mahanadi Catchment,* The Indian Geograph. J. *65*, 112–122.

RAO, Y.R., CHITTIBABU, P., DUBE, S.K., RAO, A.D., and SINHA, P.C. (1997), *Storm Surge Prediction and Frequency Analysis for Andhra Coast of India,* Mausam *48*, 555–566.

SIELECKI, A. (1968), *An Energy-conserving Difference Scheme for the Storm Surge Equations,* Mon. Weather Rev. *96*, 150–156.

(Received March 2, 2004; accepted May 14, 2004)
Published Online First: May 25 2005